Radiative recombination processes of the many-body states in multiple quantum wells

R. Cingolani and K. Ploog
Max-Planck-Institut für Festkörperforschung, Postfach 80 06 65, D-7000 Stuttgart 80, Federal Republic of Germany

A. Cingolani,* C. Moro, and M. Ferrara
Dipartimento di Fisica, Università degli Studi di Bari, I-70100 Bari, Italy
(Received 20 February 1990)

The radiative recombination processes of the electron-hole plasma in a series of GaAs/$Al_xGa_{1-x}As$ multiple-quantum-well (MQW) heterostructures have been studied by means of space-resolved high-excitation-intensity luminescence and optical-gain spectroscopy. The spontaneous electron-hole plasma emission dramatically changes depending on the actual MQW heterostructure configuration, which determines the degree of optical confinement in the epilayer. MQW heterostructures consisting of 100 quantum wells or grown on thick barrier layers, exhibit a saturation of the spontaneous emission and high stimulated-emission efficiency. Heterostructures consisting of few quantum wells exhibit the usual high-energy broadening of the luminescence due to the progressive filling of the subbands in the well. Statistical arguments on the photon-mode distribution inside the optical cavity of a semiconductor laser qualitatively account for the observed spectral features. The results of space-resolved luminescence show that the emission spectra of highly excited quantum wells are mostly given by the spectral superposition of the electron-hole plasma emission from the center of the excited region and of excitonic luminescence originating from the lateral region of the excited spot, where the carrier density is lower. These findings are explained by a simple diffusion model taking into account the drift of carriers in the plasma. The optical-gain spectra of suitably designed heterostructures allow us to determine the band-gap renormalization as a function of density of the photogenerated carriers. Additional important information on the ground-level parameters of the electron-hole plasma in GaAs quantum wells is obtained by a line-shape analysis of the optical-gain spectra using an interband recombination model.

I. INTRODUCTION

The exploration of multiple-quantum-well (MQW) semiconductor lasers has introduced important improvements as compared with conventional heterostructure lasers, namely "band-gap engineering" for tunable emission wavelengths, lower stimulation threshold, and superior room-temperature performance. As a consequence, a great deal of effort has been devoted to the investigation of the interacting many-body states in low-dimensional semiconductor structures, in order to understand the physical mechanisms underlying the radiative recombination processes in MQW's.[1] From the theoretical point of view, these studies have led to the identification of several characteristic features of the two-dimensional (2D) electron-hole plasma (EHP), including the effects of the reduced dimensionality on the screening of the Coulomb interaction and on the band-gap renormalization,[2] the effects of the Pauli exclusion principle on the carrier band filling and on the excitonic phase-space filling,[3] and the large excitonic enhancement due to the increasing electron correlation in the presence of a high-density carrier population in the MQW's.[4] From the experimental point of view, the counterparts of these effects have been investigated, with special attention paid to GaAs MQW's, by means of luminescence (see, e.g., Ref. 4–13) and optical transmission experiments in the excite-and-probe configuration.[14–17] Most of the photoluminescence data obtained from highly photoexcited MQW's have indicated the progressive filling of the higher-energy quantized states. This filling results in characteristic broadening on the high-energy side of the emission spectra when the density of photogenerated electron-hole (e-h) pairs is increased.[6,8–13] In addition, stimulated emission has been observed at energies corresponding to the $n=1$ and 2 states in photopumped quantum-well structures.[6,8,9,11]

In contrast to these observations, other experiments on highly photoexcited GaAs MQW's have shown a sharp emission band arising about 10 meV below the fundamental $n=1$ heavy-hole exciton transition, which has also been ascribed to an EHP emission.[7,16,17] This assignment is consistent with the results of pump-and-probe absorption experiments carried out either in the picosecond time domain[14] or under stationary conditions.[15] The measurements have revealed distinct absorption–to–optical-gain crossovers (corresponding to the edge of the renormalized energy gap and at the chemical potential of the EHP absorption spectrum), occurring at energies below the fundamental $n=1$ intersubband optical transitions.

In this paper we present the results of a systematic investigation of the EHP radiative recombination in GaAs/$Al_xGa_{1-x}As$ MQW structure under intense quasistationary photoexcitation. The aim of this study is

twofold: First, to study the recombination processes in the degenerate quasi-2D carrier system, and second, to get detailed information on the physical mechanisms underlying the stimulated-emission processes in these heterostructures. We have performed photoluminescence, space-resolved luminescence, and optical-gain measurements under stationary high-intensity excitation on a specially designed set of samples. Our results allow us to establish a direct correlation between the configuration of the MQW structure and the optical properties of the electron-hole plasma confined in the potential well. Different manifestations of the characteristic EHP luminescence can be observed depending on the degree of confinement of the plasma in the heterostructure. In addition, we demonstrate that the carrier diffusion within the layer plane strongly affects the characteristic line shape of the EHP luminescence. A theoretical description of the optical-gain spectra resulting from the optical amplification of the spontaneous luminescence quantitatively accounts for the observed spectral features, and it also provides information on the ground-level parameters of the two dimensional EHP (i.e., renormalized energy gap, chemical potential, and carrier temperature).

The paper is organized as follows: In Sec. II we present the configuration and optical properties of the investigated GaAs/$Al_xGa_{1-x}As$ MQW heterostructures and briefly describe the experimental details. In Sec. III A we discuss the EHP spontaneous and stimulated-emission spectra and their dependence on the MQW configuration. The results of the space-resolved luminescence measurements are presented in Sec. III B. In Sec. III C we discuss the optical-gain–spectroscopy data. A quantitative evaluation of the ground-level parameters of the two-dimensional electron-hole plasma in the investigated material system is given by means of a theoretical analysis of the optical-gain spectra. Finally, in Sec. IV we summarize the main results and draw our conclusions.

II. EXPERIMENT

The radiative-recombination processes have been studied in GaAs/$Al_xGa_{1-x}As$ MQW heterostructures grown by molecular-beam epitaxy (MBE) on undoped (001)-oriented GaAs substrate. The configurations of the samples are summarized in Table I. The MQW samples have nearly identical structural parameters, but an increasing number of periods (N). Our experiments show that the number of wells constituting the heterostructure strongly affects the emission properties of the MQW under high photogeneration rate, and it also determines the performance of the laser action up to room temperature. The investigated set of MQW's with $10<N<200$ also includes a sample which consists of 25 periods grown on a 1-μm-thick $Al_{0.36}Ga_{0.64}As$ layer on the GaAs buffer sample (No. 6). The structural parameters of the investigated samples have been determined independently by high-resolution double-crystal x-ray-diffraction measurements.

The sample specimens have typical surface dimensions of 10×7 mm^2. In some cases small optical cavities of size 150 μm$\times2$ mm have been cleaved. This allowed us to reduce self-absorption losses in the unexcited region, and also provided efficient feedback for the optical amplification of the spontaneous emission, due to the high internal reflectivity of the cleaved facets.

The excellent quality of the investigated sample has been established by means of photoluminescence-excitation (PLE) and photoluminescence (PL) measurements. In all the samples we observe sharp excitonic peaks with typical full widths at half maximum (FWHM's) of 1.5 meV at low temperature and 8 meV at room temperature. In sample 6 an additional sharp exciton peak from the $Al_{0.36}Ga_{0.64}As$ barrier layer was observed at 625 nm in the low-temperature PLE spectrum.

In all the measurements the luminescence was excited by a N_2-laser-pumped dye laser operating at the emission wavelength of 570 nm (i.e., in the continuum of the absorption for the investigated set of samples) and at 10 Hz repetition frequency. The maximum peak power density obtained by tightly focusing the beam over a spot of 100 μm diameter was $I_0=2$ MW/cm^2. The pulse duration was about 5 ns; therefore all the measurements have been performed under quasistationary conditions. The detection system consisted of a 0.6-m monochromator equipped with a fast-response photomultiplier tube and boxcar amplifier.

Two main configurations have been adopted for studying the spontaneous-emission and optical-gain processes of the photogenerated EHP in the quantum wells (QW's), respectively. First, the spontaneous luminescence was collected in the backward direction from the excited sample surface. In particular, the spatially resolved luminescence was performed by collecting the backscattered luminescence at different distances (d) from the center of

TABLE I. Configuration of the investigated GaAs/$Al_xGa_{1-x}As$ MQW samples. L_z and L_b are the well and barrier thicknesses, respectively, x is the Al mole fraction of the $Al_xGa_{1-x}As$ barrier, and N is the number of quantum wells.

Sample no.	L_z (nm)	L_b (nm)	N	x	Barrier layer
1 ("6436")	10.6	15.8	10	0.36	no
2 ("6438")	10.6	15.8	25	0.36	no
3 ("6432")	10.6	15.8	50	0.36	no
4 ("6433")	10.6	15.8	100	0.36	no
5 ("6347")	10.0	15.8	200	0.35	no
6 ("6439")	10.6	15.8	25	0.36	1 μm $Al_{0.36}Ga_{0.64}As$

the excited spot. A spatial resolution ranging between 20 and 50 μm was obtained by scanning an enlarged image of the sample surface (magnified by a factor of 10) across the entrance slit of the monochromator by means of micrometric displacements of the collecting lens. Under these conditions the spatial resolution is therefore controlled directly by the slit width, which, in turn, depends on the PL efficiency of the investigated sample. Second, the optical amplification of the spontaneous emission was studied in a configuration with the incident laser beam parallel to the [001] growth axis and the detection along the MQW plane in the [110] direction. Quantitative measurements of the optical gain have been performed by varying the excited stripe length on the sample and using the one-dimensional optical amplificator approximation.[18]

III. RESULTS AND DISCUSSION

A. Spontaneous and stimulated emission

The results of the photoluminescence measurements elucidate the characteristic EHP emission arising from quasi-2D semiconductors under intense photoexcitation. The luminescence efficiency grows proportional to the number of periods constituting the GaAs/$Al_xGa_{1-x}As$ MQW heterostructure. We observe two different manifestations of the EHP emission under identical excitation conditions depending on the MQW configuration. Samples with more than 100 periods ($N > 100$) exhibit a sharp emission band peaked in the low-energy tail of the E_{11h} transition. This band shows a red shift as a function of the excitation intensity, and, above a certain threshold intensity, a sharp stimulated emission is obtained (analogous to Refs. 7, 16, and 17). Conversely, GaAs/$Al_xGa_{1-x}As$ MQW samples with $N < 100$ do not show any separate EHP emission, but only the progressive filling of the high-energy states in the QW, resulting in the well-known high-energy emission.[6,8-13] In these cases the luminescence is peaked around the intersubband transition energies and does not show any red shift with the excitation intensity. A distinct improvement of the emission performance, resulting in very efficient stimulated emission at room temperature, can be achieved by growing the MQW on a thick $Al_xGa_{1-x}As$ barrier. This configuration is realized in sample 6, which exhibits by far the highest luminescence efficiency of the investigated set of samples.

The characteristic luminescences are exemplified in the spectra of Figs. 1(a), 1(b), and 2. In Fig. 1(a) we show the emission spectra of MQW no. 6 obtained at different excitation intensities. The spectra were recorded in the back scattering configuration, and they are thus virtually unaffected by the self-absorption in the crystal. At the lowest power density only the sharp excitonic E_{11h} line around 799.0 nm is present. With increasing excitation intensity a new band (S) arises in the low-energy tail of the E_{11h} line. This band grows superlinearly with respect to the excitonic line [see the inset of Fig. 1(a)] and shows a red shift of about 15 meV in the intensity range between $0.1I_0$ and I_0. In addition, weak contributions to the luminescence spectra from the GaAs buffer (E_b band) and from the thick $Al_xGa_{1-x}As$ barrier layer can be identified around 820 and 630 nm, respectively. These weak features indicate an efficient carrier trapping in the MQW active layers. When we further increase the incident power density, the S band becomes dominant, as depicted in Fig. 1(b). Very similar spectra have been obtained from samples composed of a large number of QW's, i.e., with a total MQW thickness much larger than the penetration depth of the exciting radiation (samples 4 and 5).

When we decrease the number of the QW's in the sample or remove the barrier layer, we no longer observe the separate S emission band. A typical example of this situation is shown in Fig. 2, where the luminescence spectra from sample 1 (10 QW's) are depicted. Although these spectra are recorded under identical conditions as the spectra of Figs. 1(a) and 1(b) and from GaAs quantum wells of identical well (L_w) and barrier (L_b) widths, the emission line shapes are totally different. First, a strong emission arises on the high-energy side of the E_{11h} band as the excitation intensity is increased, which clearly reflects the effect of the Pauli exclusion principle on the photogenerated carrier population. Second, a strong luminescence from the GaAs buffer layer is observed. This clearly indicates that a large portion of the exciting light is not absorbed by the MQW, owing to the penetration depth of the radiation being longer than the MQW thickness.

The impact of the discussed luminescence features on the stimulated-emission spectra of the investigated samples is exemplified in Figs. 3(a) and 3(b). The spectra are obtained in the configuration with the exciting laser beam perpendicular to the sample edge. In Fig. 3(a) the stimulated-emission spectra at 10 K of sample 5 with 200 periods are shown for pumping-power densities ranging from $0.002I_0$ to I_0 (4 kW/cm^2 up to 2 MW/cm^2). At an excitation intensity of about $0.005I_0$, the S band arises at 802.3 nm (1.545 eV), about 6 meV below the E_{11h} excitonic emission, and it becomes dominant at the highest excitation levels. The S linewidth narrows down to 2 meV at $0.01I_0$ (20 kW/cm^2). When the excitation level is increased, its emission intensity grows exponentially up to $0.05I_0$ (100 kW/cm^2). Then it broadens and saturates as I_0 is further increased up to 2 MW/cm^2. An appreciable red shift of the S line of about 5 meV is observed by increasing the excitation intensity. The buffer-layer emission, located at 820 nm, is observed only at the maximum power intensity. The dependence on the pump intensity for both the S and E_{11h} bands is shown in the inset of Fig. 3(a). The stimulated emission S depends exponentially on the excitation intensity, while the excitonic emission exhibits a sublinear dependence.

The stimulated-emission spectra of sample 6 are very similar to those measured in sample 5. In particular, in sample 6 the stimulated-emission threshold is about 1 order of magnitude lower than that of sample 5 and the stimulated S band is present even at very low excitation intensity. The lowest-excitation-intensity thresholds for the occurrence of stimulated emission measured in these two samples are 0.2 kW/cm^2 for sample 6 and 11.2

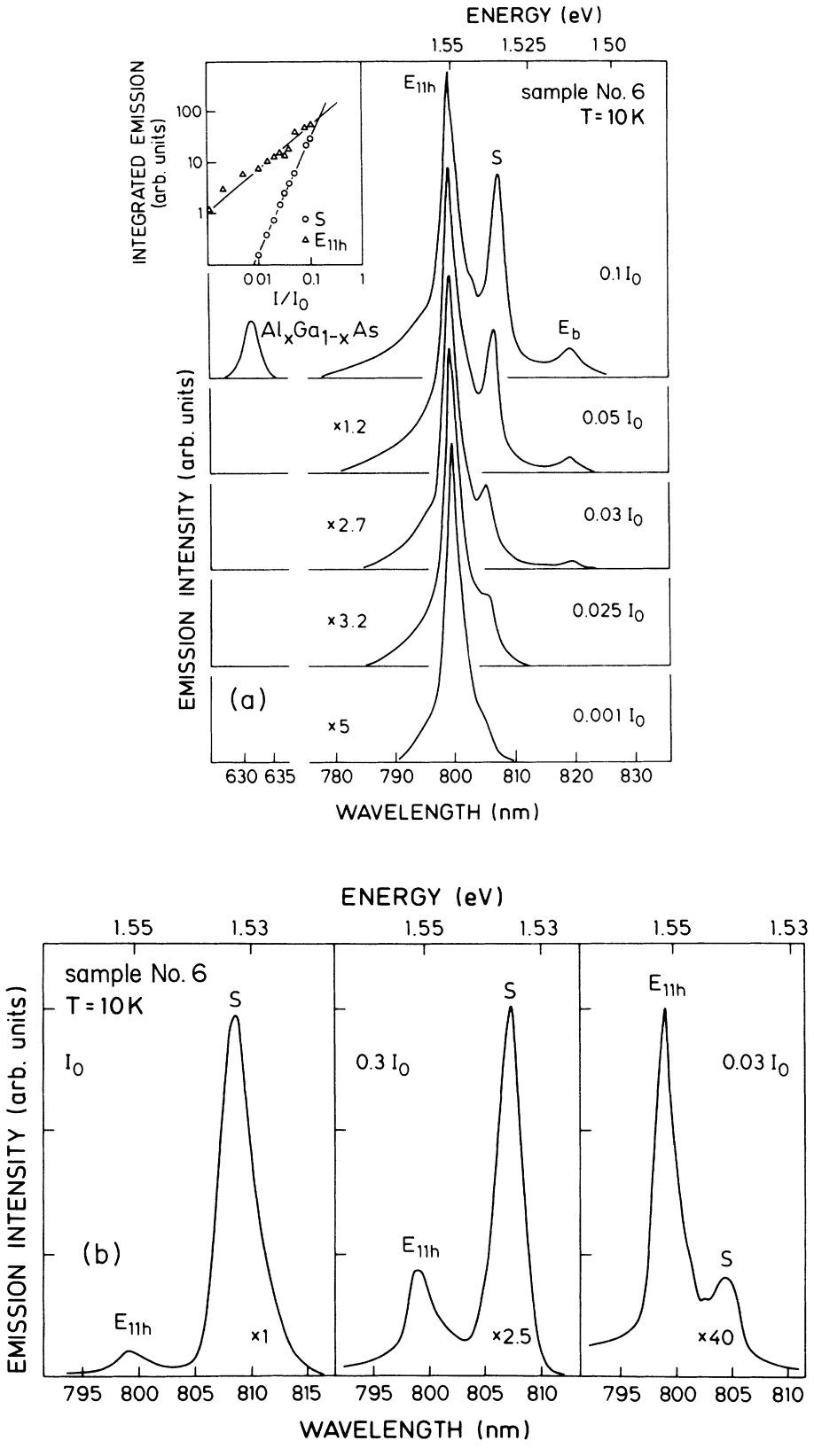

FIG. 1. (a) Spontaneous-emission spectra of sample 6 (25 wells and $Al_{0.36}Ga_{0.64}As$ barrier layer) recorded in backscattering geometry at 10 K under excitation intensity $0.001I_0 < I < 0.1I_0$. For a better comparison, the spectra have been multiplied by a constant factor indicated in the figure. In the inset the dependence on pumping intensity for both E_{11h} and S is shown. (b) Same as in (a), but for excitation intensity $0.3I_0 < I < I_0$.

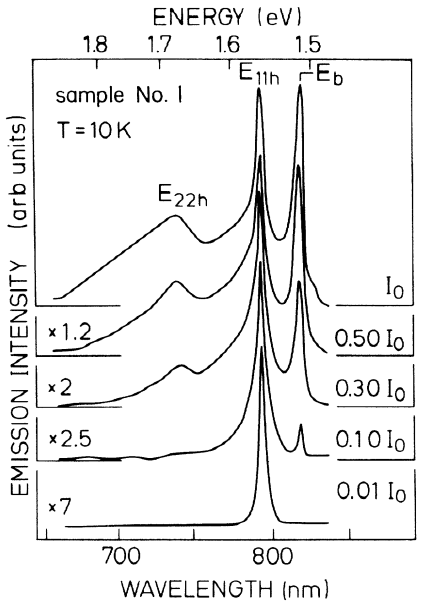

FIG. 2. Emission spectra of sample 1 (10 wells) obtained under the same excitation conditions as those of Fig. 1.

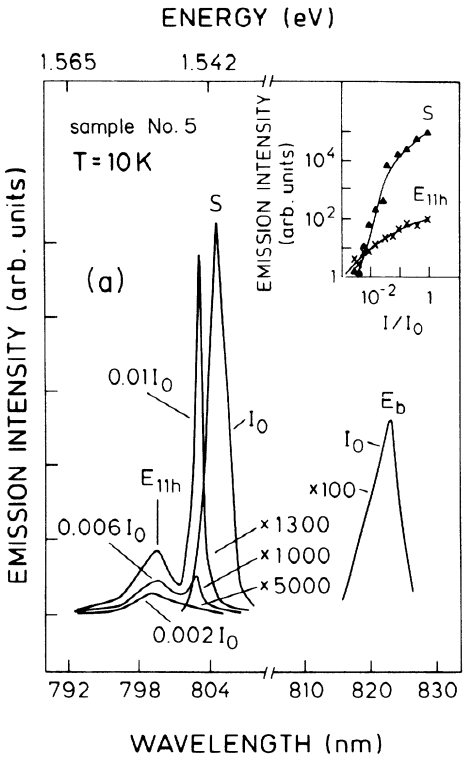

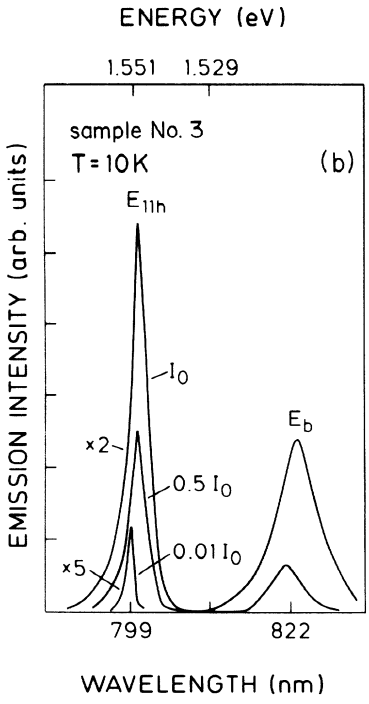

FIG. 3. (a) Stimulated-emission spectra of sample 5 (200 wells) recorded at 10 K under different pumping intensities. The spectra are multiplied by a constant factor given in the figure. The inset shows the dependence on pumping intensity for both E_{11h} (crosses) and S (triangles). (b) Emission spectra of sample 3 (50 wells) recorded at 10 K under different pumping intensities. The spectra are multiplied by a constant factor given in the figure.

kW/cm^2 for sample 5 at 10 K, while at room temperature (RT) we obtain 10 kW/cm^2 for sample 6 and 480 kW/cm^2 for sample 5.

In Fig. 3(b) we show the emission spectra at 10 K of the MQW sample with 50 periods (sample 3) recorded at different excitation intensities from $0.01I_0$ to I_0 (20 kW/cm^2 to 2 MW/cm^2). No stimulated emission is observed from this sample up to the maximum excitation intensity. At the lowest pumping level an emission line is located at the energy position of the E_{11h} transition. When increasing the excitation intensity to I_0, the band grows weakly superlinear. It broadens with the pump intensity and shifts slightly towards the red.

Comparison of the data of Figs. 1–3 clearly reveals the important result that samples consisting of a few quantum wells without any confining $Al_xGa_{1-x}As$ barrier exhibit a broad EHP spontaneous emission. This emission is characterized by a density-dependent band-filling line shape which originates from the radiative recombination of electrons and holes populating the higher-energy subbands. The integrated emission intensity from these MQW configurations grows linearly with the excitation intensity and at a rate nearly twice that measured for the E_{11h} exciton emission. On the contrary, MQW configurations with $N > 100$ or with a confining $Al_xGa_{1-x}As$ barrier do not show any band-filling emission, but only the sharp S band on the low-energy side of the fundamental E_{11h} transition. The S band grows exponentially with the excitation intensity [see inset of Fig. 1(a)], indicating that optical amplification is established in the crystal. In both cases the formation of a dense electron-hole plasma in the MQW heterostructure must be invoked in order to explain the observed luminescence spectra. Other radiative-recombination mechanisms responsible for the S emission, like exciton-exciton or exciton-electron scattering processes,[19] can be excluded

on the basis of magneto-optical measurements performed under similar excitation conditions. Details of the magneto-optical results will be given in a forthcoming paper.[20]

The different luminescence properties obtained from MQW heterostructures consisting of either a few or a large number of wells and/or having a confining barrier layer can be explained on the basis of the photon distribution in the optical cavity of a semiconductor-laser structure with cleaved reflecting faces.[21] The number of quanta M in a single mode of the radiation field within the active layer is given by

$$M=\frac{R_{\rm sp}(E)}{N(E)/t_m-R_{\rm st}(E)}\ , \tag{1}$$

where $R_{\rm sp}(E)$ and $R_{\rm st}(E)$ are the rates of spontaneous and stimulated transitions at different energies E, respectively, $N(E)$ is the number of modes per unit volume and unit-energy interval, and $1/t_m$ is a term representing the photon losses in a mode of energy E due to self-absorption in the crystal, transmission, and scattering (Q factor of the mode). For modes with high losses (small Q factor), the value of $R_{\rm st}(E)$ can hardly approach that of $N(E)/t_m$. Therefore, the denominator of Eq. (1) is large, resulting in a small number of quanta of energy E in the given mode. This condition is usually achieved when the spontaneous luminescence emitted in the active layer can be absorbed by the underlying GaAs buffer layer due to the poor optical confinement of the structure. On the contrary, for modes with low losses (large Q factor) even a small $R_{\rm st}$ rate can approach the $N(E)/t_m$ factor, resulting in a vanishing denominator for Eq. (1), i.e., in a very large number of photons in the low-loss mode. In this case a sharp stimulated-emission peak appears in the luminescence spectrum of the crystal. In a phenomenological way this means that all the radiative-recombination transitions in the crystal occur through the lasing channel owing to the large Q value of the corresponding fraction of modes. The limit for the existence of a large amount of stimulated emission is given when the condition $F(E)/t_m=R_{\rm st}(E)$ is fulfilled in Eq. (1). By using the existing relation between the spontaneous- and stimulated-emission rates,[21] this condition becomes

$$R_{\rm sp}(E)[1-\exp(E-\Delta F)/kT]=N(E)/t_m\ , \tag{2}$$

where ΔF is the difference in electron and hole quasi-fermi-levels of the EHP, and kT is the thermal energy of the carriers. From Eq. (2) we deduce that the condition at which $R_{\rm st}(E)$ approaches $N(E)/t_m$ also establishes an upper limit for the steady-state Fermi level of the electron-hole plasma, thus giving a saturation of the spontaneous emission. Under these conditions, any increase of the emission rate occurs in the stimulated-emission channel.

The mechanisms discussed explain our experimental findings. MQW structures in which optical losses in the active layer are large do not show optical amplification, and the EHP spontaneous luminescence exhibits the characteristic band-filling behavior. This is the case for the MQW samples with thin active layers (samples 1–3), in which self-absorption of the spontaneous luminescence occurs in the GaAs buffer layer (leakages of photogenerated carriers in the underlying substrate in samples whose active layer thickness is shorter than the penetration depth of the exciting radiation should also be considered an additional loss mechanism). In fact, in these samples saturation of the spontaneous emission can hardly occur, and the characteristic EHP luminescence manifests itself mainly through the well-known band-filling spectra. However, the MQW heterostructures with a thick active layer provide a large optical confinement of the emitted luminescence, which reduces the model losses in the cavity, thus resulting in the sharp stimulated-emission band. In fact, in the MQW samples with a large number of wells (samples 4 and 5) the effective penetration depth of the exciting radiation reasonably involves only the first 20 periods. Therefore, the underlying slabs act like an optical confinement layer characterized by the average refractive index:[22]

$$n_{\rm av}=[Nn_wL_w+(N-1)n_bL_b]/[NL_w+(N-1)L_b]\ , \tag{3}$$

where $n_w=3.6$ and $n_b=3.6-0.7x$ are the refractive indexes of GaAs and $Al_xGa_{1-x}As$, respectively. In the case of samples 5 and 4, Eq. (3) results in a refractive-index discontinuity of the order of 4%, which is sufficient to give some optical confinement of the luminescence. In the case of sample 6, this effect is enhanced by the presence of the thick $Al_xGa_{1-x}As$ barrier layer, which provides a very efficient optical confinement and prevents self-absorption of the spontaneous luminescence and carrier leakage into the GaAs buffer layer. The observation of the stimulated S band in the luminescence spectra from the thick MQW configuration can therefore be explained as a consequence of the reduction of the losses of the spontaneous-emission photons in the MQW active layer, resulting in the strong reduction of the denominator of Eq. (1). Such a condition is mainly achieved in the edge of the renormalized energy gap, where the self-absorption is strongly reduced. Therefore, the stimulated emission is expected to occur at an energy below the fundamental E_{11h} transition and to red-shift with increasing excitation density. This red shift follows the density-induced band-gap shrinkage, as we do indeed observe for the S band in the spectra of Figs. 1(a), 1(b), and 3(a). In addition, as previously discussed, in these MQW configurations we do not observe the characteristic band-filling emission line shape due to the saturation of the spontaneous emission. It is worth noting that this result is confirmed by the observation of a shortening of the luminescence decay time above the stimulation threshold. Göbel *et al.*[8] have shown that in the presence of stimulated emission the increase of the excitation intensity leads to a further increase of the optical amplification and to a reduction of the carrier lifetime, which indicates the saturation of the spontaneous emission.

B. Space-resolved luminescence

Another important feature of the photoluminescence spectra discussed in the preceding subsection is that the

diffusion of the photogenerated carriers along the QW basal plane strongly affects the line shape of the emission spectra under high excitation intensity. The careful study of the emission spectra by means of spatially resolved luminescence measurements allows us to demonstrate that the line shape of the EHP luminescence observed at high carrier density is derived from a spectral superposition of excitonic and free-carrier luminescence originating from different lateral regions of the crystal where the actual *e-h* density can be totally different.

Under stationary conditions it is expected that the photogeneration of a dense EHP in the crystal results in the ionization of excitons due the screening of the Coulomb interaction. Several theoretical investigations of this subject[2] predict that at an *e-h*–pair density of the order of 10^{11} cm^{-2} the excitons are ionized, and this gives rise to radiative recombination at the edge of the renormalized band gap. On the other hand, the observed EHP luminescence spectra clearly exhibit a peak located at the exciton transition, even at very high excitation intensities, when the photogenerated *e-h* density is considerably larger than 10^{12} cm^{-2}. This can be clearly observed not only in the spectra of Figs. 1 and 2, but also in many experimental results published previously.[9–13] The use of spatially resolved luminescence reveals that this phenomenon is due to the spectral superposition of different radiative-recombination processes originating in different lateral regions of the crystal where the actual carrier densities differ strongly. This important aspect is exemplified in the spectra of Figs. 4 and 5.

In Fig. 4 we depict the spatially resolved luminescence of sample 6, taken at several different distances d from the center of the excited spot. The lateral resolution is 20 μm in this case. As shown in a previous paper,[19] the EHP emission can be observed only in the center of the excited spot, where the actual carrier density is the largest. By displacing the detection far away from the center of the spot, we observe an overall decrease of the total integrated emission intensity and a dramatic decrease of the EHP emission, which reduces to about 10% of the $d=0$ value at a distance of about 500 μm from the spot center. However, the E_{11h} line does not show significant changes, even 700 μm away from the spot center. From these findings we deduce that the exciton luminescence comes from the unexcited part of the samples surrounding the excitation region, where the carrier density is strongly reduced. Similar effects are also observed for the band-filling luminescence of MQW sample 2 with the small number of wells shown in Fig. 5. Again, we observe a sharp excitonic emission in the space-integrated measurement which overlaps the band-filling spectrum originating from free-carrier recombination involving different subbands. By selecting the center of the spot with a pin hole of 200 μm diameter, we observe the sharp decrease of the exciton recombination, while no changes occur in the free-carrier emission spectrum.

The observation of luminescence up to 800 μm away from the excited spot (whose diameter is about 100 μm) indicates a strong in-plane EHP expansion. Many theoretical models have been proposed to explain the carrier drift in dense electron-hole–plasma states, and re-

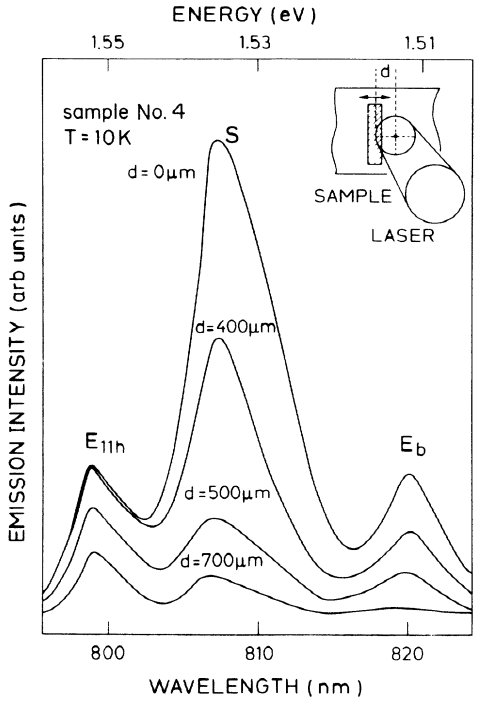

FIG. 4. Spatially resolved luminescence of sample 6 (25 wells and $Al_{0.36}Ga_{0.64}As$ barrier layer) at 10 K under the maximum excitation intensity recorded at different distances d from the exciting spot.

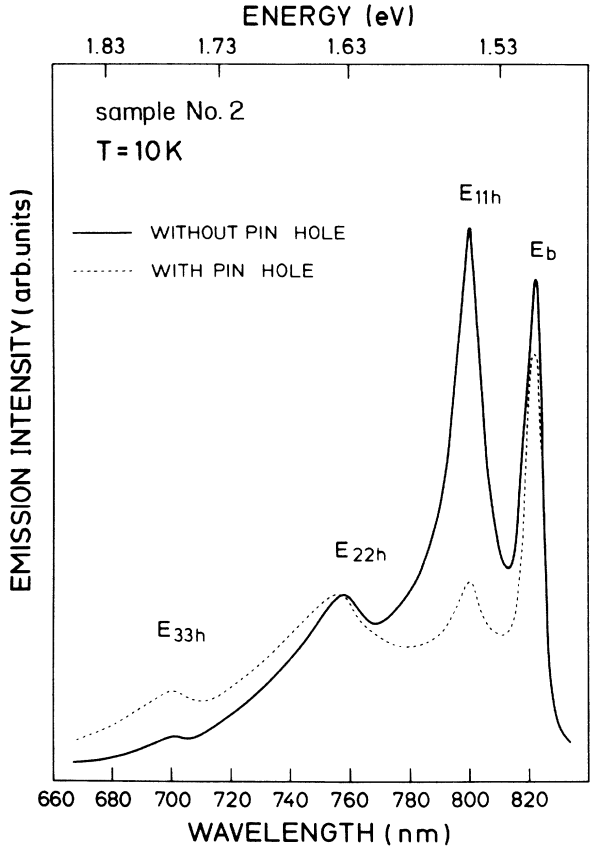

FIG. 5. Emission spectra of sample 2 (25 wells) obtained by collecting the luminescence through a pin hole of 200 μm diameter placed in the center of the excited spot (dashed line), and without a pin hole (solid line).

cently a direct measurement of the expansion of a relatively-low-density EHP in GaAs quantum wells has been reported.[23] The main conclusion of those studies is that the carrier transport is thermodiffusive and occurs along the layer plane. The measured drift of the order of tens of μm has been monitored with a time-resolved probing technique. In our experiments, however, the photogeneration rate is under quasistationary conditions and the detection is time integrated. The observation of the large EHP expansion is probably related to some additional drift mechanism which depends on the *e-h* density. In fact, the purely diffusive drift length of carriers in GaAs is of the order of $\sqrt{D\tau}=3.5$ μm (D is the GaAs diffusion coefficient equal to 120 cm^2/s,[23] and τ is the electron recombination time of the order of 1 ns), which cannot account for our experimental observation. A possible mechanism which explains the observed strong carrier expansion is increase of the Fermi pressure in the nonequilibrium EHP.[24] Under these conditions the continuity equation for the charge density $n(x,t)$ in space and time of the EHP can be written as

$$\frac{dn}{dt}=D\frac{d^2n}{dx^2}+v\frac{dn}{dx}+g(x)-\frac{n}{\tau}\ , \tag{4}$$

where $g(x)$ is the carrier-photogeneration rate, v is the drift velocity of the plasma, and τ is the recombination time. The analytical solution of Eq. (4) is a Gaussian carrier distribution centered at $x(t)=vt$, with amplitude $[g(0)/(2\sqrt{\pi Dt})]\exp(-t/\tau)$ decreasing in time.[25] It is therefore evident that this additional carrier-drift mechanism displaces the carrier distribution at distance vt from the center of the excited spot. This effect can usually be neglected at low carrier density, but it becomes important at the EHP densities involved in the present experiments. Under these conditions, we can assume a velocity of the order of the Fermi velocity for both carrier species ($v>10^7$ cm/s).[23,24] The result of this rough estimate is that the carrier distribution can easily be displaced by 100 μm from the spot within one carrier lifetime.

An additional spatial inhomogeneity in the EHP density can arise from intercarrier scattering processes which broaden the carrier distribution. The expansion and broadening of the carrier population causes an inhomogeneous carrier distribution with a density profile decreasing at large distances from the exciting spot. At the external edge of the expanding EHP region, the carrier density is hence much lower. This causes a reduction of the screening and allows for the formation of excitons at large d values. The above arguments imply that the spatial expansion and inhomogeneity of the carrier distribution strongly affect the luminescence line shape of the electron-hole plasma. The description of this effect made by means of Eq. (4) allows us to explain qualitatively most of the observed spectral features of Figs. 4 and 5.

C. Optical-gain spectroscopy

The results of the photoluminescence measurements discussed in the preceding subsections evidence the close relation existing between the actual configuration of the MQW heterostructure and the radiative-recombination processes in the confined electron-hole plasma. An efficient optical amplification of the spontaneous emission can easily be achieved in MQW heterostructures having a large number of wells or grown on a barrier layer. In order to account quantitatively for the optical amplification capability of the samples investigated, we have performed optical-gain measurements by varying the length of the exciting stripe on the sample surface.

In Fig. 6 we show the unsaturated optical-gain spectra of MQW sample 5 with 200 periods obtained at 10 and 300 K. The gain bands are located almost at the energy of the S band, showing a maximum g value of about 1600 and 30 cm^{-1} at 10 and 300 K, respectively. Similar optical-gain spectra have been obtained from sample 4 ($N=100$), which shows a less efficient optical amplification at low temperature. A very efficient optical gain is, however, observed in sample 6 (grown on an $Al_xGa_{1-x}As$ barrier layer), as expected from the conclusion of Sec. III A.

The unsaturated optical-gain spectra of sample 6 obtained at 10 K for different photogeneration rates are depicted in Fig. 7. The electron-hole–pair densities n are calculated from the width of the gain spectra according to

$$n=(kT/\hbar\omega)\sum_j m_j\ln\{1+\exp[(F_h-E_j)/kT]\}\ , \tag{5}$$

where j indicates the light- and heavy-hole contributions, E_j are the subband energies, and F_h is the quasi-Fermi-level of the hole population (a similar formula is valid for the electrons). The maximum gain value is peaked almost at the energy of the S band and it reaches 5600 cm^{-1} at 10 K and becomes 250 cm^{-1} at 300 K.

Inspection of the data of Fig. 7 implies that the energy position of the maximum g value is almost independent of

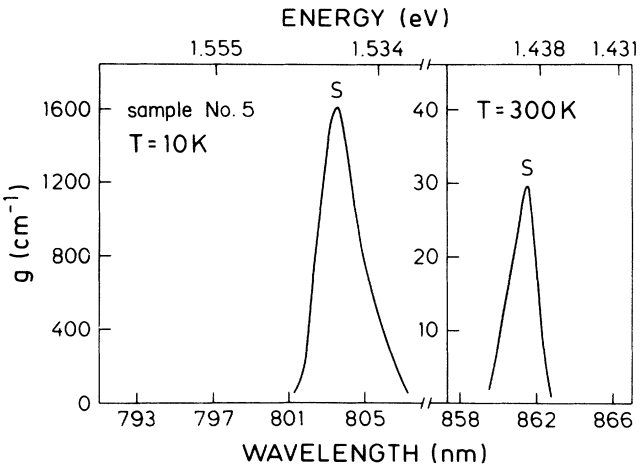

FIG. 6. Unsaturated optical-gain spectra of sample 5 (200 wells) obtained at 10 and 300 K. The spectrum at 300 K has been multiplied by a constant factor indicated in the figure.

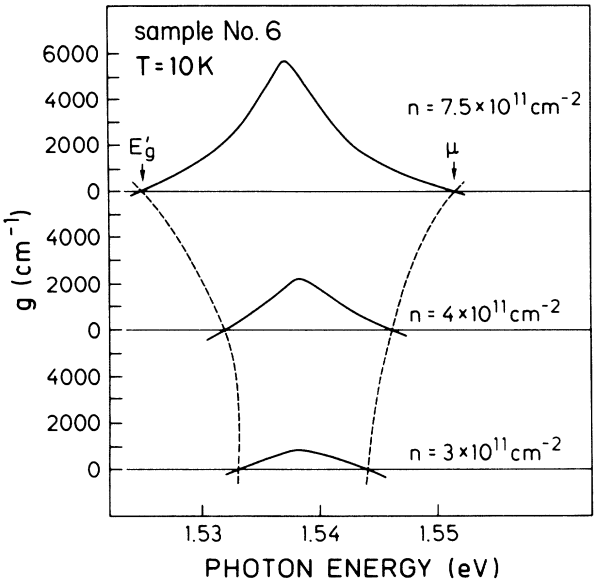

FIG. 7. Unsaturated optical-gain spectrum of sample 6 (25 wells and $Al_{0.36}Ga_{0.64}As$ barrier layer) obtained at 10 K and different carrier densities n. Neglecting broadening effects in the spectra, the crossovers indicate the energy positions of the renormalized energy gap (E_g' in the low-energy side) and of the chemical potential (μ in the high-energy side). The dashed lines are guides for the eyes, indicating the density-dependent shift of the crossovers.

the e-h density, whereas the crossover points (where the optical gain changes to absorption) shift in opposite directions. In particular, by increasing the carrier density, the chemical potential μ (the high-energy crossover) shifts to higher energy and the renormalized energy gap E_g' (the low-energy crossover) shifts to lower energy. The estimated band-gap shrinkage ranges from 27 meV at 3×10^{11} cm^{-2} to 36 meV at 7×10^{11} cm^{-2}. These values are in quantitative agreement with the experimental results of Weber *et al.*[15] obtained in pump-and-probe absorption experiments, and they are only slightly larger than the theoretical values calculated by Haug *et al.* and Das Sarma *et al.* in Ref. 2. The present results indicate that the band-gap renormalization can easily be studied by means of simple luminescence measurements in samples having a configuration suitable for high optical gain. This opens up the possibility of systematic experimental investigations of the well-width dependence of the band-gap renormalization without experimental complications arising from the application of pump-and-probe methods.

More detailed information on the ground-level parameters of the EHP in the QW can be obtained by the line-shape analysis of the optical-gain spectra. The calculation of the two-dimensional EHP luminescence line shape can be performed by using a band-to-band recombination model accounting for momentum conservation. In addition, energy- and density-dependent lifetime broadening is taken into account.[22] The quantitative analysis has been carried out on the unsaturated optical-gain spectra measured in sample specimens whose dimensions are comparable with the excited stripe length (about 100 μm). In Fig. 8 we show the results of a least-squares fit carried out on the experimental unsaturated optical-gain spectrum obtained from a small optical cavity (150 μm$\times$2 mm surface size) cleaved from sample 6. The gain curve peaks almost at the energy of the S band and exhibits a maximum g value of 7860 cm^{-1}. The optical-gain spectrum $g(\hbar\omega)$ is given by[22]

$$g(\hbar\omega)=\begin{cases} I(g',\hbar\omega), & \hbar\omega<F_e \\ I(g',\hbar\omega)+g'(\hbar\omega), & \hbar\omega>F_e \end{cases} \tag{6}$$

with

$$I(g',\hbar\omega)=\int_{E_g}^{F}\frac{g'(E)}{\Gamma(E)/2\pi}\,\frac{dE}{\Gamma^2(E)/4+(\hbar\omega-E)^2} \tag{7}$$

and

$$g'(E)=(A/2)\sum_n\sum_v(4\pi m_0/\hbar^2)\times H(E-E_g-E_n^c-E_n^v)(f_n^c-f_n^v)\,, \tag{8}$$

where A is a constant, f_n^c and f_n^v are the occupation factors of the nth subband, $H(x)$ is the Heaviside unit-step function, Γ is the broadening parameter, and the other symbols have their usual meanings. The calculation reproduces the experimental spectrum very well, with best-fit parameters $\Gamma=20$ meV and the renormalized band gap $E_g'=1.532$ eV. The total quasi-Fermi-level of the three-component electron–heavy-hole and –light-hole population obtained by the fitting procedure amounts to 17 meV, which corresponds to a carrier density of 4.7×10^{11} cm^{-2} at the effective temperature of 20 K. From these data we derive a band-gap reduction of 29 meV at the e-h density of 4.7×10^{11} cm^{-2}, in agreement with the results of Fig. 7. These calculations demonstrate that the unsaturated optical gain of the highly excited

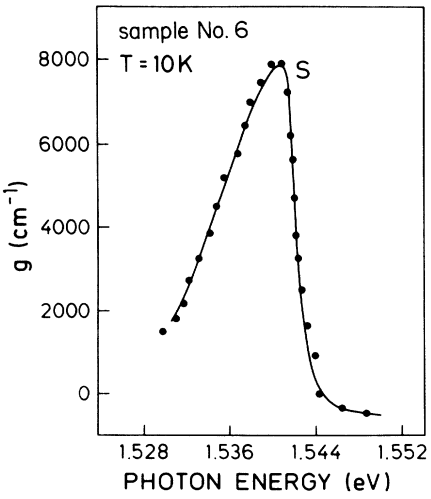

FIG. 8. Experimental (dots) and theoretical (solid line) unsaturated optical-gain spectra of an optical cavity cleaved from sample 6 (25 wells and $Al_{0.36}Ga_{0.64}As$ barrier layer).

quantum wells originates from the optical amplification of the luminescence emitted by interband transitions (i.e., radiative-recombination processes by free carriers in the EHP). In addition, the application of the simple theoretical model of Eqs. (6)–(8) allows us to determine the ground-level parameters of the EHP state in the QW, which provides important information on the carrier distribution responsible for laser action in the semiconductor. It should be noted that this interband recombination model describes the observed optical-gain spectra well in a wide range of *e-h* densities and/or lengths of the excited stripe on the sample surface. Deviations from the interband recombination mechanism are observed only at very large lengths of the excited stripe when the optical gain saturates.

IV. CONCLUSIONS

We have discussed several fundamental aspects of the radiative-recombination processes occurring in highly excited quantum wells. The systematic investigation of the EHP luminescence and optical gain in a set of $GaAs/Al_xGa_{1-x}As$ MQW heterostructures of different configuration allows us to draw the following conclusions: First, the characterized luminescence of the electron-hole plasma in MQW samples depends on the actual heterostructure configuration. In particular, band-filling luminescence caused by the progressive population of higher-energy subbands in the well is observed in MQW samples consisting of only a few periods. Conversely, sharp EHP luminescence occurring below the fundamental E_{11h} interband transition is observed in MQW samples consisting of 100 periods or more or grown on a thick $Al_xGa_{1-x}As$ barrier layer. The latter configuration is also most advantageous in obtaining stimulated emission. This apparent discrepancy in the manifestation of the EHP luminescence is due to the degree of optical confinement of the luminescence inside the heterostructure. A qualitative explanation of this effect has been given in terms of statistical distribution of photon modes inside the optical cavity of a semiconductor laser. In thick MQW heterostructures providing high optical confinement of the luminescence, the spontaneous emission saturates at relatively low excitation intensity, resulting in sharp stimulated emission at an energy where the self-absorption losses are negligible (i.e., around the edge of the band gap). On the contrary, in thin MQW samples providing low optical confinement the saturation of the spontaneous emission hardly occurs, resulting in the well-known band-filling luminescence arising on the high-energy side of the E_{11h} transition. These findings allow us to understand apparent discrepancies existing in the literature among the results of different spectroscopic investigations of the EHP in MQW heterostructures.

The second interesting result concerns the correct interpretation of the EHP luminescence line shape obtained from the experimental spectra. Our measurements of the space-resolved luminescence indicate that in standard luminescence experiments the EHP luminescence is given by the spectral superposition of free-carrier and excitonic emission originating in different regions of the crystal surface, where the density of carriers is totally different. In particular, the free-carrier luminescence arises from the center of the excited spot where the carrier density is the highest, while the excitonic emission originates far away from the spot center, where the actual carrier density is reduced by the strong EHP expansion. At the carrier densities of our experiments this phenomenon can be described by a diffusion model taking into account the carriers' drift in the nonequilibrium plasma.

Finally, the ground-level parameters of the electron-hole plasma confined in the MQW heterostructure (renormalized band gap, chemical potential, and carrier temperature) have been determined by studying the optical-gain spectra of the EHP. The dependence of the optical gain on the *e-h*–pair density provides quantitative information on the band-gap renormalization in the presence of a dense carrier population. The ground-level parameters of the carrier distribution have been determined by calculating the optical-gain line shape with an interband recombination model. The results of the calculations confirm that the main radiative-recombination channel is the interband free-carrier recombination in the dense electron-hole plasma.

ACKNOWLEDGMENTS

We gratefully acknowledge A. Fischer and M. Hauser for expert help with sample growth and R. Muralidharan for preparation of the optical cavities. We thank E. O. Göbel for many illuminating discussions and suggestions, and L. Tapfer for x-ray-diffraction studies. This work has been partially supported by the Bundesministerium für Forschung und Technologie (Federal Republic of Germany) and by the National Research Council of Italy (under Special Project "Tecnologie Elettroniche").

---

*Deceased.

[1]For a recent review, see S. Schmitt-Rink, D. S. Chemla, and D. A. B. Miller, Adv. Phys. **38**, 89 (1989).

[2]D. A. Kleinman and R. C. Miller, Phys. Rev. B **32**, 2266 (1985); D. A. Kleinman, *ibid.* **32**, 3766 (1985); S. Das Sarma, R. Jalabert, and S. R. Eric Yang, *ibid.* **39**, 5516 (1989); H. Haug and S. Schmitt-Rink, J. Opt. Soc. Am B **2**, 1135 (1985); S. Schmitt-Rink and C. Ell, J. Lumin. **30**, 585 (1985).

[3]S. Schmitt-Rink, D. S. Chemla, and D. A. B. Miller, Phys. Rev. B **32**, 6601 (1985).

[4]S. Schmitt-Rink, C. Ell, and H. Haug, Phys. Rev. B **33**, 1183 (1986).

[5]N. Holonyak, Jr., R. M. Kolbas, R. D. Dupuis, and P. D. Dapkus, IEEE J. Quantum Electron. **QE-16**, 170 (1980).

[6]Z. Y. Xu, V. G. Kreismanis, and C. L. Tang, Appl. Phys. Lett. **44**, 136 (1983).

[7]H. Q. Le, B. Lax, B. A. Vojak, and A. R. Calawa, Phys. Rev. B **32**, 1419 (1985).

[8]E. O. Göbel, R. Höger, J. Kuhl, H. J. Polland, and K. Ploog, Appl. Phys. Lett. **47**, 781 (1985).

[9]S. Borestain, D. Fekete, M. Vofsi, R. Sarfaty, E. Cohen, and Arza Ron, Appl. Phys. Lett. **50**, 442 (1987).
[10]G. Trankle, H. Leier, A. Forchel, H. Haug, C. Ell, and G. Weimann, Phys. Rev. Lett. **58**, 419 (1987).
[11]R. Cingolani, Y. Chen, and K. Ploog, Nuovo Cimento D **10**, 529 (1988); R. Cingolani, M. Ferrara, M. Lugarà, C. Moro, Y. Chen, F. Bassani, J. Massies, and F. Turco, Europhys. Lett. **7**, 651 (1988).
[12]M. Colocci, M. Gurioli, M. Querzoli, A. Vinattieri, and F. Fermi, Nuovo Cimento D (to be published).
[13]G. Bongiovanni, J. L. Staehli, and D. Martin, Phys. Rev. B **39**, 8359 (1989).
[14]C. V. Shank, R. L. Fork, R. Yen, J. Shah, B. J. Greene, A. C. Gossard, and C. Weisbuch, Solid State Commun. **47**, 981 (1983).
[15]C. Weber, C. Klingshirn, D. S. Chemla, D. A. Miller, J. E. Cunningham, and C. Ell, Phys. Rev. B **38**, 12 748 (1988).
[16]N. Peyghambarian and H. M. Gibbs, J. Opt. Soc. Am. B **2**, 1215 (1985).
[17]J. A. Levenson, I. Abram, R. Raj, G. Dolique, J. L. Oudar, and F. Alexandre, Phys. Rev. B **38**, 13 443 (1988).
[18]K. L. Shaklee, R. E. Nahory, and R. F. Leheny, J. Lumin. **7**, 248 (1973).
[19]R. Cingolani, K. Ploog, G. Peter, R. Hahn, E. O. Gobel, C. Moro, and A. Cingolani Phys. Rev. B **41**, 3272 (1990).
[20]R. Cingolani, K. Ploog, M. Potemsky, and J. C. Maan (unpublished).
[21]G. Lasher and F. Stern, Phys. Rev. A **133**, 553 (1964).
[22]E. Zielinski, H. Schweizer, S. Hausser, R. Stuber, M. H. Pilkuhn, and G. Weimann, IEEE J. Quantum Electron. **QE-23**, 969 (1987).
[23]K. T. Tsen and H. Morkoç, Phys. Rev. B **34**, 6018 (1986); K. T. Tsen, O. F. Sankey, G. Halama, and Shu-Chen Y. Tsen, *ibid.* **39**, 6276 (1989), and references therein.
[24]K. M. Romanek, H. Nather, J. Fisher, and E. O. Göbel, J. Lumin. **24/25**, 585 (1981).
[25]See H. Mathieu, *Physique des semiconducteurs et des composants electroniques* (Masson, Parts, 1987), Chap. 9, p. 453 (in French).